Prediction of ASDEX Upgrade disruptions using discriminant analysis

Y. Zhang[1, 2], G. Pautasso[2], O. Kardaun[2], G. Tardini[2], X.D. Zhang[1]
and the ASDEX Upgrade Team[2]
[1]*Institute of Plasma Physics Chinese Academic of Sciences, Hefei, China*
[2]*Max Planck Institute for Plasma Physics, EURATOM Association, Garching, Germany*

1. Introduction

There has been a growing interest in a physically based approach to disruption prediction in recent years. Disruptions have different physical causes. The prediction method proposed here is aimed at developing different criteria to predict different classes of disruptions. The approach is expected to explore the recognition algorithms related to physical laws and well-established empirical behaviour, which will be suitable for the prediction of disruptions in ITER.

A large number of disruptions (325 shots) that occurred in the years 2005-2009 of operation in ASDEX Upgrade (AUG) have been analysed with the purpose of identifying their causes, precursors and finding their predictive criteria. All disruptions selected for this study were in the flat-top phase or within the first 100 ms of the ramp-down phase of discharges, where the plasma conditions were $I_p > 0.7$ MA and $\kappa > 1.5$. The results of this analysis are presented in the following sections.

2. Classes of disruptions

The time traces of plasma parameters have been visually analysed. According to the last mechanism leading to them, disruptions are roughly divided into four classes: (1) vertical displacement disruption (VDD), (2) edge cooling disruption (ECD) [1], (3) impurity accumulation disruption (IAD) [2], (4) β limit disruption (BLD) and others with undefined cause. In AUG, the second class represented the majority of the disruptions in the past [2] and the same situation arose also in the years 2005-2007. In 2008 and 2009, the VDDs occurred more frequently and amounted to almost 40% of the disruptions. In 2008, both VDDs and ECDs represented 80% of the disruptions, but the percentage decreased to 60% in 2009, due to the increasing number of the latter two classes of disruptions.

3. Detection of the VDDs

A VDD is defined as a disruption following the plasma vertical displacement. A total of 106 VDDs (33%) are found in the analysed data set of AUG, half of which were caused by a large plasma equilibrium perturbation. The reason why VDDs happened so frequently recently in AUG has not been clarified yet. A threshold value for the plasma vertical displacement is used to detect the VDDs. The threshold is searched for in the interval 0.005 - 0.1 m, and the 57 VDDs and 62 non-VDDs are used as training discharges to obtain the optimum value. Figure 1 shows that the threshold value of 0.07 m is appropriate, with which 55 VDDs can be detected correctly, and 4 discharges are wrongly recognized as VDDs.

4. Discriminant analysis for ECDs

The cooling of the plasma edge is well known as mechanism leading to disruptions [1]. In AUG, it is found that 146 disruptions (45%) were caused by this reason in the last four years.

Discriminant analysis [3, 4] is applied to develop a criterion to predict this type of disruptions.

Discriminant analysis is performed on two groups of the database, which consists of 3900 observations extracted from 75 ECDs and 4687 observations from 896 non-disruptive shots. An observation is a vector containing the logarithm of the 10 global plasma parameters listed in table 1. The covariance matrices are estimated with the set of observations and used to derive a discriminant function. It allows to calculate the 'probabilities' that an observation belongs to each one of the two groups, and then the group membership of the observation is determined according to its largest probability. The performance of the discriminant function can be evaluated by the error rate, which is defined as the average rate of the mis-classifications of the observations in each group.

An analysis seeking two, three, four and more variables from the preliminary 10 variables in the database, whose linear combination (L) and quadratic combination (Q) minimize the error rate, is performed. The selection is based on the stepwise discriminant analysis using SAS [6]. Table 2 shows the variable entering at each step and the final combinations used. The variable H98(y, 2) (see [5]) is expected to be helpful to forecast the occurrence of a ECD, but it has hitherto been hardy applied to on-line disruption prediction, owing to its complex dependence on plasma parameters. Therefore, the contribution of H98(y, 2) is investigated separately in order to clarify how important it is. Figure 2 shows that the error rates decrease as the number of variables used increases. Apparently, the first three variables play important roles in the classification of observations. When the variable $\ln n_e/n_{GW}$ is used alone to classify the observations, it gives a high error rate. However it decreases the error rates by a factor of 2 if it is used together with $\ln l_i$. Also it is less correlated with $\ln l_i$ than $\ln U_{loop}$, ln H98(y, 2) and $\ln P_{frac}$. The ln H98(y, 2) can improve slightly the performance of the discriminant function, and the quadratic combination of variables works better than the linear one.

However, the performance testing should be refined beyond the mis-classifications of the observations to include the factor that makes the prediction of disruption in a particular shot useful or not. Therefore, the original 73 (= N_{disr}) edge cooling disruptions and 111 (= N_{ndisr}) non-disruptive discharges are used to test the four combinations once more. Each discriminant function allows to calculate the disruptive probability at each time point during the flat-top phase of a discharge. We assume that if the disruptive probability is larger than a given alarm level (threshold probability), then a disruption alarm is generated in a discharge. A disruption alarm is defined as successful alarm (SA) when it is triggered in the time interval [t_{disr} – 500 ms, t_{disr} - 2ms]; a false alarm (FA) is produced when a disruption alarm is activated in a non-disruptive discharge or more than 1s before a disruption; a disruption alarm more than 500 ms but less than 1s before a disruption is considered a premature alarm (PA); a missed disruption (MD) occurs when a disruption is not recognized or the alarm is activated less than 2 ms before a disruption. Moreover, a success-to-failure ratio (SFR) is defined as

$$SFR = \frac{SA / N_{disr}}{[(FA_{disr} + FA_{ndisr}) / (N_{disr} + N_{ndisr})] * c + (MD / N_{disr}) * (1 - c)}$$

where the denominator is the failure rate and c = 0.5 is assumed here. For each discriminant function, the SFR and the premature alarm rate $PAR = PA / N_{disr}$ depend on the alarm level, and they are plotted in figure 3. The alarm level for each function is optimized by maximizing

SFR. Then the performances of the four discriminant functions can be compared under their own optimum alarm levels. A bigger SFR represents a better performance, besides the PAR is small. Table 3 summarizes the details of their optimum performance. It is seen that the 6 variables ($\ln l_i$, $\ln n_e/n_{GW}$, $\ln U_{loop}$, $\ln P_{frac}$, $\ln \beta_N$, $\ln \delta$) combined with linear functions can provide the best prediction performance in the discharges, and that the variable of $\ln$H98(y, 2) does not improve the performance any more in whatever linear combination or quadratic combination.

Another factor that can influence the performance of the discriminant function is the covariance structure. Fixing the above 6 variables, five structures based on different assumptions for the relation between the covariance matrices of two groups are investigated. Specially, the common principle component and proportional covariance models (see [7]) give a similar error rate (about 7%) as does the linear model mentioned above. For the practical application, the following linear discriminant function is proposed, which is derived from L1 with optimum alarm level of 0.895.

$$(U'_{loop})^{1.01} * l_i^{0.96} * (n_e/n_{GW})^{0.48} * P_{frac}^{0.19} * \beta_N^{-0.07} * \delta^{-0.04} = 7.13$$

5. Prediction performance for extra shots

To confirm the performance of VDD and ECD predictive criteria, an extra test is performed by using extra shots in 2009 campaign, which are not used in the training process. The extra shots consists of 39 VDDs, 31 ECDs, 34 other types of disruptions and 106 non-disruptive discharges. As a result, the threshold value of 0.07 m can detect 97% of VDDs correctly and yield a failure rate of 2.98%; The linear discriminant function allows to recognize 94% of ECDs successfully and generates a failure rate below 2%. Actually, the discriminant analysis has been performed in the same way on the impurity accumulation disruptions and β limit disruptions, but no proper predictive criteria were found. We deduce that the global plasma parameters used do not allow to discriminate between these two types of disruptions and non-disruptive phases.

6. Conclusion

The discriminant analysis on ECDs indicates that only a few variables are really important for the disruption prediction, and a simple function is able to predict this type of disruptions. The method can quantify the predictive capability of each plasma parameters. The predictive criterion performs quite well, while it avoids some drawbacks of the black box approach to disruption prediction.

References

[1] F.C. Schueller, Plasma Phys. Control. Fusion 37 (1995) , A135

[2] G. Pautasso, 25th EPS Conference, Vol. 22C(1998), 520-523

[3] Otto J. W. F. Kardaun, Classical Methods of Statistics, Springer, 205-247

[4] L. Giannone, Plasma Phys. Control. Fusion 46 (2004) , 835

[5] ITER Physics Basis, Nucl. Fusion 39 (1999), Ch.2, 2203-2211

[6] SAS Institute Inc, NC, SAS/STAT User's Guide, Version 9.2 (2008)

[7] S-PLUS 7, Guide to Statistics, Vol 2, 83-104

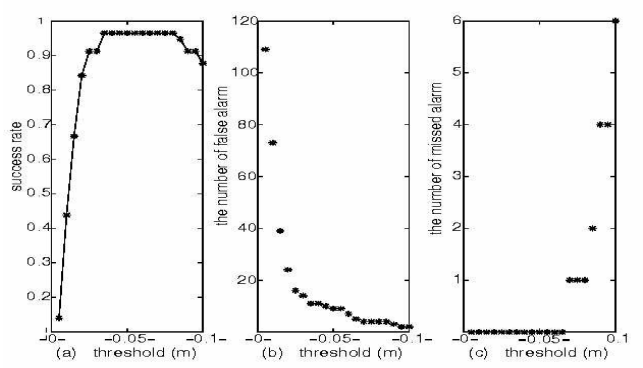

Figure 1. (a) The success rate of VDD prediction depends on the threshold for the vertical displacement; (b) the false alarms decrease as the threshold increases; (c) the missed alarms are generated after 0.065 m.

Table 1. The 10 plasma variables.

Variable	Range
l_i	0.67 - 2.11
n_e/n_{GW}	0.04 - 1.91
$H98$(y, 2)	0 - 2
U_{loop}	- 4.70 - 8.14
[(1)] P_{frac}	0 - 6
β_N	0.01 - 4.34
q_{95}	2.58 - 7.22
δ	0.09 - 0.39
κ	1.2 - 1.94
[(2)] $ikCAT$	1- 4

(1) $P_{frac} = P_{rad}/(P_{inp} - \frac{dW_{tot}}{dt})$

(2) $ikCAT$, plasm configurations; 2,4 = upper, lower divertor; 1,3= inner, outer limiter.

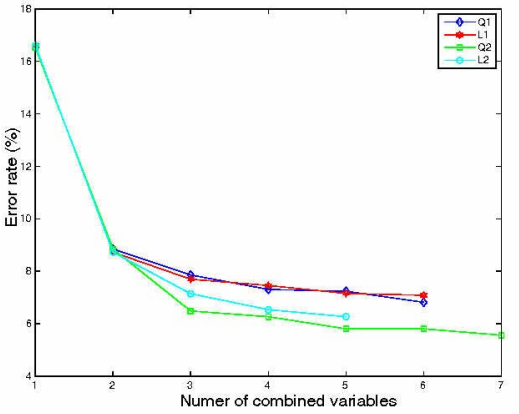

Figure 2. Error rates of four discriminant functions versus the number of variables.

Table 2. List of variables used in the quadratic (Q1 and Q2) and linear (L1 and L2) discriminant functions.

	Variables
Q1	$\ln l_i$, $\ln n_e/n_{GW}$, $\ln U'_{loop}$, $\ln P_{frac}$, $\ln \beta_N$, $\ln q_{95}$
L1	$\ln l_i$, $\ln n_e/n_{GW}$, $\ln U'_{loop}$, $\ln P_{frac}$, $\ln \beta_N$, $\ln \delta$
Q2	$\ln l_i$, $\ln n_e/n_{GW}$, $\ln H98(y,2)$, $\ln \beta_N$, $\ln P_{frac}$, $\ln q_{95}$, $\ln U'_{loop}$
L2	$\ln l_i$, $\ln n_e/n_{GW}$, $\ln H98(y,2)$, $\ln U'_{loop}$, $\ln P_{frac}$

* $lnU'_{loop} = \ln(U_{loop} + 4.8)$

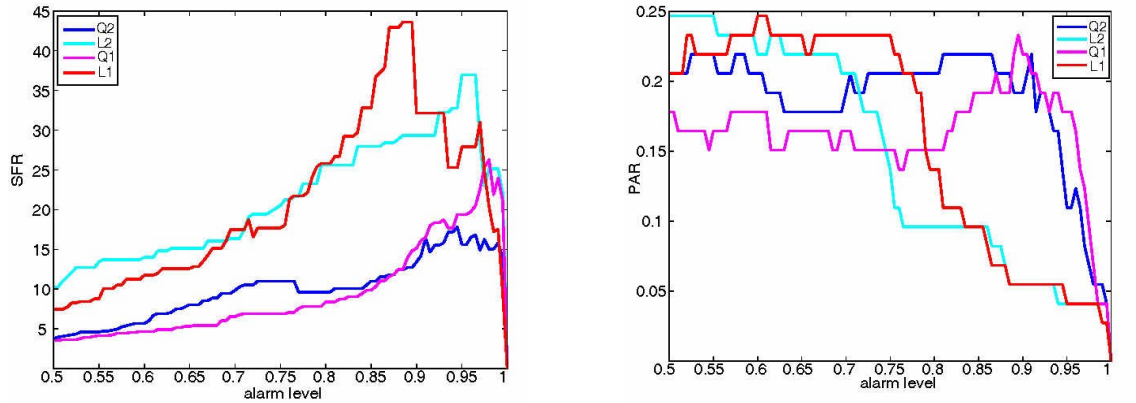

Figure 3. Dependence of the success-to-failure rate (SFR) and of the premature alarm rate (PAR) on the alarm level for the four discriminant functions (Q1, Q2, L1, L2)

Table 3. The best prediction results of each discriminant function.

	N_{disr}=73				N_{ndisr}=111	Failure rate (%)	SFR	Alarm level
	SA	MD	PA	FA_{disr}	FA_{ndisr}			
Q2	55	3	10	5	3	4.23	17.82	0.945
L2	66	0	3	4	5	2.45	36.97	0.950
Q1	60	1	5	7	2	3.13	26.25	0.980
L1	65	1	4	3	2	2.04	43.57	0.895